# Nek8445, a protein kinase required for microtubule regulation and cytokinesis in *Giardia lamblia*.

Kelly M. Hennessey[a], Germain C.M. Alas[a], Ilse Rogiers[b], Renyu Li[a], Ethan A. Merritt[b], Alexander R. Paredez[a]

[a]Department of Biology, University of Washington, Seattle, WA 98195; [b]Department of Biochemistry, University of Washington, Seattle, WA 98195

Corresponding author: aparedez@uw.edu

**Abstract:**

*Giardia* has 189 Nek kinases whereas humans have only 11. We previously identified Nek8445 as a potential drug target due to susceptibility to a specific class of kinase inhibitors and essential function in parasite proliferation and attachment. *Giardia* has a complex tubulin cytoskeleton that includes eight flagella and several unique microtubule arrays that are utilized for parasite attachment and facilitation of rapid mitosis and cytokinesis. The need to regulate these structures may explain the parallel expansion in the number of Nek family kinases. Here we use live and fixed cell imaging to uncover the role of Nek8445 in regulating *Giardia* cell division. We demonstrate that Nek8445 localization is cell cycle regulated and this kinase has a role in regulating overall microtubule organization. Nek8445 depletion results in short flagella, aberrant ventral disc organization, loss of the axostyle (funis), defective flagella exit and altered cell shape. The flagella exit defect is specific to the caudal flagella, which exit from the posterior of the cell, and this defect correlates with rounding of the cell posterior and loss of the axostyle. This correlation implicates a role for the axostyle in establishing *Giardia's* cell shape and guiding flagella docking. Axostyle biogenesis can now be included in the list of functions regulated by Nek family kinases.

## Introduction

The protozoan parasite *Giardia lamblia (synonymous with G. intestinalis and G. duodenalis)* infects more than 200 million people each year. The divergence of parasite protein kinases from their homologs, in humans has been identified as an opportunity for the development of new drugs (Rotella, 2012). The *Giardia* kinome (strain WB) contains 278 protein kinases, 80 of which constitute the core kinome from 49 different classes of kinases while the remainder are all Nek Kinase homologs (Manning *et al.*, 2011). The highly expanded *Giardia* Nek family contains 198 kinases, compared to only one in budding yeast, seven in *Arabidopsis*, 11 in humans, and 13 in *Chlamydomonas* (Manning *et al.*, 2011; Takatani *et al.*, 2015).

Nek kinases are named for their homology to the *Aspergillus nidulans* NIMA (never in mitosis A) kinase. Nek kinases have been shown to control mitotic entry and flagella length in other eukaryotes (O'Connell *et al.*, 2003; Bradley and Quarmby, 2005), but may also have a more general role in regulating microtubule organization (Takatani *et al.*, 2015). Nek kinases are typically more abundant in the genomes of eukaryotes that build cilia or flagella (Parker *et al.*, 2007). Notably, *Giardia* possesses four pairs of flagella that undergo a complex developmental cycle (Nohynkova *et al.*, 2006) (See Figure 1 for diagram of *Giardia* structures). As pairs of flagella do not share paired basal bodies, maintaining the identity of each flagella is complex and the regulatory mechanism remains uncharacterized (Nohynkova *et al.*, 2006). The complexity of maintaining eight flagella identities could explain the development of a greatly expanded set of Nek kinases.

Flagella positioning and identity are essential for *Giardia* cellular processes including pathogenicity. Unlike most other eukaryotes that dock their basal bodies just under the plasma membrane, *Giardia* positions its eight basal bodies between the two nuclei in the center of the cell. As a result, a significant portion of each axoneme runs through the cytoplasm of the cell before it exits and is sheathed by membrane. The portion of the axonemes running through the cell body are known as cytoplasmic axonemes, they serve as tracks for cargo trafficking (Hardin

*et al.*, 2017). Also indicating the complexity of specifying flagella identity, each flagella pair beats with a unique waveform and has a specific role in motility and the biology of *Giardia* (Lenaghan *et al.*, 2011). For example, the caudal flagella pair, which runs the length of the cell body, is thought to flex the entire body of the cell to contribute to swimming via a flipper type mechanism (Lenaghan *et al.*, 2011). The anterior and ventrolateral flagella generate power strokes for motility; while the ventral flagella, with a unique fin-like appendage, beat in a sinusoidal waveform thought to generate fluid flows beneath and around *Giardia* trophozoites (Lenaghan *et al.*, 2011; Halpern *et al.*, 2017).

In addition to four unique sets of flagella, *Giardia* has several novel microtubule structures including the ventral adhesive disc, median body, and axostyle (named funis in *Giardia)*. Each of these structures has regulated assembly and disassembly during the cell cycle that may involve Nek kinases (Smith *et al.*, 2012). The ventral disc is a complex dome shaped structure composed of approximately 100 microtubules in a one and a quarter turn helical sheet and is thought to mediate attachment through a suction cup like mechanism (Nosala *et al.*, 2018). The funis is a pair of microtubule sheets that originate at the basal bodies and run above and below the caudal flagella, branching out at the cell posterior to form a rib-like structures that lock the intracytoplasmic axonemes of the caudal and posteriorlateral flagella together (Benchimol *et al.*, 2004). The median body is a reservoir of microtubules and associated binding proteins used to support *Giardia's* rapid mitosis, which is completed in approximately 7 minutes and includes building two new ventral discs (Hardin *et al.*, 2017). Currently, little is known about how the assembly and disassembly dynamics of these structures are regulated. Moreover, *Giardia* lacks an anaphase promoting complex suggesting that kinases play an enhanced role in regulating mitotic events (Gourguechon *et al.*, 2013).

The *Giardia* Nek kinase homologs with the highest sequence identity for human Nek1 and Nek2 were previously studied (Smith *et al.*, 2012). The Nek1 homolog GlNek1 localized to the ventral disc while the Nek2 homolog GlNek2 localized to the intracytoplasmic axonemes of

the anterior flagella. Both kinases re-organize during mitosis and over-expression studies showed that GlNek1 has a role in ventral disc disassembly while GlNek2 over expression interfered with excystation (hatching from the cyst form). Other *Giardia* Nek kinases have not yet been individually studied.

Here, we report the characterization of Nek kinase GL50803_8445 (Nek8445). Nek8445 has direct orthologs (>90% sequence identity) in other *Giardia* assemblages (strains), but exhibits little similarity (30-40% sequence identity) to other Nek paralogs in the expanded *Giardia* Nek kinome. This is consistent with a functional role in *Giardia* that is both essential and distinct from that of other Nek family kinases. We previously identified this kinase as a potential therapeutic target due to the presence of a small gatekeeper residue, which makes it susceptible to a specific class of kinase inhibitors with relatively low activity against human kinases (Hennessey *et al.*, 2016). These “bumped kinase inhibitors” (BKIs) exploit the property that most mammalian protein kinases have a large gatekeeper residue that limits accessibility to a hydrophobic pocket in the active site. Various BKIs have been shown to selectively and effectively block kinase-associated processes in the life cycle of parasites such as *Toxoplasma gondii, Cryptosporidia parvum* and *Plasmodium falciparum* (Keyloun *et al.*, 2014).

Nek8445 depleted cells are severely impeded in growth, often abnormally multinucleated, and unable to maintain attachment. Our initial study of Nek8445 involved examining cells 48 hours after morpholino knockdown. Cellular organization was severely disrupted and therefore the primary defect was not apparent. However, the cytokinesis and attachment defects are potentially explained by aberrant flagella function. Unlike other eukaryotes that use an actomyosin contractile ring to drive cell division, *Giardia* utilizes its flagella to coordinate membrane trafficking into the furrow as well as propel daughter cells apart during cytokinesis (Hardin *et al.*, 2017). The flagella may also have a role in parasite attachment. It has been proposed that flows generated by the ventral flagella transit through gates in the ventral disc which can close off to lock down attachment (Dawson and Nosala,

2017). Here we examine the role of Nek8445 in *Giardia's* unique mode of cytokinesis.

## Methods & Materials

### Parasite culture

Giardia *lamblia* wild-type strain *WBC6* (ATCC 50803) cells were grown in TYI-S-33 medium supplemented with 10% bovine serum and 0.05 mg/mL bovine bile (Keister, 1983). Cells were cultured at 37° under hypoxic conditions using 15 mL polystyrene screw-cap tubes (Corning Life Sciences DL).

### Vector construction and transfection

With the exception of Rab11, the constructs used in this study were C-terminal fusions. All constructs were integrated into the genome to maintain endogenous expression levels (Gourguechon and Cande, 2011). Primer sequences and restriction enzymes are shown in Table S1. All PCR amplifications were performed using iProof DNA polymerase (Bio-Rad). Typically, an amplicon of ~ 1 kb in length that lacked the start codon was cloned in frame to a C-terminal triple-hemagglutinin epitope tag (3xHA) of the pKS_3HA_Neo or puromycin plasmid. The plasmids were linearized at a unique restriction site in the coding region of the gene of interest and ~5 µg of DNA was used to transform wild-type *Giardia*. Transformants were selected with G418 at 40 µg/mL or puromycin at 45 µg/mL.

To follow Nek8445 localization throughout mitosis and cytokinesis, the C terminus of GL50803_8445 was tagged with an 11-amino acid flexible linker and the bright fluorescent protein mNeonGreen (Allele Biotechnology). The mNG-N11-Neo vector was constructed for this purpose by amplifying mNeonGreen using the primers listed in Table S1. The PCR product was cloned into the pKS 3HA Neo vector (Gourguechon and Cande, 2011) after excising the 3HA tag with BamH1 and EcoR1.

### Live cell imaging

Cells were imaged in 35mm glass bottom dishes at 37° C under hypoxic conditions as

described in (Hardin *et al.*, 2017).

**Immunofluorescence microscopy analysis**

Fixed cell imaging was performed as described in (19). In cases where a higher mitotic index was desired, the starve and release method was utilized before fixation (20). Briefly, four-day-old past confluent cultures were inverted to loosen dead cells and the spent media was poured off and replaced with fresh media. Four hours later *Giardia* cells were pelleted at 500xg at room temperature. The pellet and remaining attached cells were fixed in PME (100 mM Pipes pH 7.0, 5 mM EGTA, 10 mM MgSO4) plus 2% paraformaldehyde, 0.025% Triton X-100, 100 µM MBS, and 100 µM EGS for 30 minutes at 37°C. Cells were again pelleted, washed, resuspended with PME, and adhered to poly-L-lysine (Sigma-Aldrich) coated cover-slips. Cells were permeabilized in PME + 0.1% Triton X-100 for 10 minutes then washed 2X with PME + 0.1% Triton X-100 and blocked for 30 minutes in PMEBALG (PME + 1% BSA, 0.1% NaN3, 100 mM lysine, 0.5% cold water fish skin gelatin (Sigma Aldrich, St. Louis, MO).

Cells were stained with rabbit anti-giActin antibody 28PB+1 (21) and mouse monoclonal anti-HA (Clone HA7, Sigma-Aldrich) both diluted 1:125 in PMEBALG and incubated over-night. After three subsequent washes with PME + 0.05% Triton X-100, cells were incubated with Alexa-488 goat anti-mouse and Alexa-555 goat anti-α-rabbit (Sigma- Aldrich, St. Louis, MO) (diluted 1:150 in PMEBALG) for 1 h. Cells were washed three times with PME + 0.05% Triton X-100. The coverslips were mounted with ProLong Gold or Prolong Diamond anti-fade plus DAPI, (ThermoFisher Scientific, Rockford, IL). Fluorescence deconvolution microscopy images were collected as described (19). A minimum of 200 cells were examined with at least 30 imaged per experiment. Structured illumination images were acquired on an OMX SR (GE Healthcare).

**Morpholino knockdown and growth assays**

Trophozoites were cultured until 85-100% confluence, iced for 30 minutes to detach, spun down at 500xg for 5 minutes, and media was replaced with 1.0 mL fresh *Giardia* growth medium. Cells

and cuvettes were chilled on ice. Lyophilized morpholinos listed in Table S1 (Gene Tools, LLC, Philomath, OR) were resuspended in sterile water and 30 µL of a 100 mM morpholino stock was added to 300 µL of cells in a 4 mm cuvette. We used Gene Tools, LLC standard morpholino as a negative control. Cells were electroporated (375V, 1000 µF, 750 Ohms, GenePulser Xcell, Bio-Rad, Hercules, CA) and returned to growth media. See (22) for a detailed protocol.

**Western blot analysis**

*Giardia* trophozoites were harvested after chilling cultures on ice for 30 minutes. After detachment, cells were pelleted at 700xg, washed once in HBS (HEPES buffered saline), then resuspended in 300 µL of lysis buffer (50 mM Tris pH 7.5, 150 mM NaCl, 7.5% Glycerol, 0.25 mM CaCl2, 0.25 mM ATP, 0.5 mM DTT, 0.5 mM PMSF, 0.1% Triton X-100, Halt 100X Protease Inhibitor Cocktail (ThermoFisher Scientific), then sonicated. The lysate was cleared by centrifugation at 10,000xg for 10 minutes at 4°C and then boiled in 2x Laemmli Sample Buffer (Bio- Rad). After SDS-PAGE, samples were transferred to PVDF membrane (Immobilon-FL) following the manufacturers' directions. Primary polyclonal rabbit anti-glActin 28PB+1 (21), monoclonal anti-HA mouse HA7 antibodies (IgG1; Sigma-Aldrich), 6-11B-1 anti-acetylated tubulin (IgG2b), DMA1 anti-alpha Tubulin (IgG1, Sigma-Aldrich), were diluted 1:2500 in blocking solution (5% dry milk, 0.05% Tween-20 in TBS). Secondary isotype specific anti-mouse Alexa-555 or anti-rabbit Alexa-647 antibodies (Molecular Probes) were used at 1:2500. Horseradish peroxidase-linked anti-mouse or anti-rabbit antibodies (Bio-Rad) were used at 1:7,000. Multiplexed immunoblots were imaged on a Chemidoc MP (Bio-Rad) and signals were quantitated using ImageJ (23).

**Scanning Electron Microscopy**

For scanning electron microscopy (SEM) analysis, trophozoites were pelleted at 700xg for 7 minutes, fixed with 2.5% glutaraldehyde in 0.1 M phosphate buffered saline (PBS), pH 7.4 and incubated for 1 h. After fixation, cells were pelleted again at 700xg for 7 minutes and washed

twice and resuspended in PBS. Cells were adhered to poly-L-lysine (Sigma-Aldrich) coated coverslips for 15 minutes then washed three times for 5 minutes with PBS and post-fixed in 1% $OsO_4$ for 1 h. Cells were washed three times 5 minutes each with $dH_2O$, dehydrated in alcohol, dried to critical point with $CO_2$, sputter coated with gold and analyzed on JEOL JSM-840A SEM.

**Accession numbers**

**Genes/proteins**

**Nek8445: GL50803_8445; Flagella Exit Site Protein: GL50803_8855, Rab11: GL50803_1695, Actin: GL50803_40817; δ-giardin: GL50803_86676**

## Results

### Nek8445 function is required for cytokinesis

The initial observation that Nek8445 plays a role in cytokinesis was based on analysis of Nek8445 depleted cells fixed and analyzed 48 h after treatment with translation-blocking antisense morpholinos (14). These cells were abnormally multinucleate (more than 2 nuclei) with a roughly corresponding increase in flagella number. The flagella appeared mis-organized; however, since there was an abnormal number of flagella and nuclei, it was not clear if the observed cytokinesis defects were a secondary result of cellular disorganization. We recently developed methods for long-term 4D DIC time-lapse imaging to follow *Giardia* trophozoites through the cell cycle (Hardin *et al.*, 2017). We sought to film Nek8445 depleted cells undergoing cytokinesis to test for changes in the timing of events and gain insight into the underlying defect that leads to failed cytokinesis. We initially examined Nek8445 depleted cells from 20 - 26 h after morpholino treatment as in our previous study of *Giardia* cytokinesis. However, the majority of these cells had already failed cytokinesis or were abnormally organized (not shown). Therefore, we decided to examine cells from 8 - 14 h after knockdown as most cells at this time point displayed typical organization as assessed by DIC imaging.

Western blotting indicated that morpholino treatment had reduced Nek8445 levels by 41% at the midpoint of the experiment (12 hours or ~1.5 cell cycles after morpholino treatment; Figure 2A). Upon initiation of cytokinesis the cleavage furrow often failed to progress (Figure 2B, Video S1). Under our assay conditions, approximately 89% of control cells completed cytokinesis within two minutes as previously reported (Hardin *et al.*, 2017). In contrast, only 13% of Nek8445 depleted cells completed cytokinesis within two minutes. Additionally, 48% of Nek8445 depleted cells never completed cytokinesis compared to just 4.5% non-completion observed for the control cells (Figure 2C). Remarkably, this cell division defect is stronger than the phenotype of any cytoskeleton or membrane trafficking component previously studied (Hardin *et al.*, 2017), suggesting a central regulatory role for Nek8445 in coordinating cytokinesis.

**Nek8445 localization is cell cycle regulated**

We previously reported that Nek8445-3HA localized to the plasma membrane and perinuclear ER in interphase cells (Hennessey *et al.*, 2016). Many cell cycle regulated proteins, including NEK kinases, change their localization during mitosis (Smith *et al.*, 2012). To follow Nek8445 localization throughout the cell cycle in live cells, the C-terminus of Nek8445 was tagged with the green fluorescent protein, mNeonGreen (Shaner *et al.*, 2013), generating Nek8445-mNeonGreen (Nek8445-mNG). This construct was integrated into the genome to ensure endogenous expression levels (Gourguechon and Cande, 2011). In Nek8445-mNG interphase cells, the fusion protein localized to the cell cortex and around both nuclei, matching the previously reported pattern for Nek8445-3HA (Hennessey *et al.*, 2016). At the initiation of mitosis, Nek8445-mNG translocated from the cell cortex to become concentrated around the two nuclei and along the flagella with some concentration at the tips (Figure 3A; Video 2). During cytokinesis Nek8445-mNG appeared to remain associated with portions of the anterior, caudal, and ventrolateral cytoplasmic axonemes.

To confirm association of Nek8445 with the cytoplasmic axonemes of flagella during mitosis and cytokinesis, we co-localized Nek8445-3HA and tubulin in fixed cells (Figure 3B). Indeed,

Nek8445-3HA generally co-localized with the intracytoplasmic axonemes of flagella including the nascent flagella that act as tracks for delivering membrane to the cleavage furrow (Hardin *et al.*, 2017).

We previously established that membrane trafficking is required to support furrow progression in *Giardia* (Hardin *et al.*, 2017). The block in furrow progression resulting from Brefeldin A treatment is similar to the defects in cytokinesis observed when Nek8445 is depleted Figure 2B (Hardin *et al.*, 2017) . Therefore, we asked if Nek8445 and Rab11 might have a functional relationship. Co-localization of HA-Rab11 with Nek8445-mNG revealed that while both proteins translocate from the plasma membrane to the intracytoplasmic axonemes during mitosis and cytokinesis, they were rarely seen to be on intracytoplasmic axonemes at the same time (Figure S1). Therefore, it is unlikely that Nek8445 is regulating membrane trafficking associated with furrowing. Instead, Nek8445 may have a role in regulating axoneme function, which is required for force generation during cytokinesis (Hardin *et al.*, 2017).

**Nek8445 depleted cells have short flagella and lack median bodies**

The microtubule cytoskeleton plays a major role in establishing *Giardia's* unique shape and in generating forces for driving cells apart during cytokinesis (Hardin *et al.*, 2017). Defects in microtubule regulation could account for defects in cell division. Therefore, we examined tubulin staining in Nek8445 depleted cells (Figure 4A). We observed that ~35% (n>300) of the Nek8445 depleted cells had short flagella and either round or oval-shaped cell bodies (Figure 4A and 4B). We also noticed that the axonemes of Nek8445 depleted cells appeared to stain more crisply while ventral disc staining was often reduced. The immunofluorescence localization was performed with the anti-acetylated α-tubulin antibody 6-11B-1 which is known to recognizes K40 acetylation and stain all known microtubule based structures in *Giardia* (Nohynkova *et al.*, 2006; Halpern *et al.*, 2017). The altered staining suggested that either the acetylation levels or microtubule array organization have been perturbed by Nek8445 depletion. Microtubule acetylation is thought to soften microtubules so that they are more flexible and able to resist

mechanical stress (reviewed in (Janke and Montagnac, 2017)). Notably, human Nek3 has been shown to regulate tubulin acetylation levels (Chang *et al.*, 2009). Therefore, we questioned whether Nek8445 has a role in regulating tubulin acetylation which could account for the observed defects in cell shape and microtubule-based processes.

To differentiate between changes in acetylation or overall microtubule organization, we co-stained cells with the anti-α-tubulin antibody DM1A and the anti-acetylated α-tubulin antibody 6-11B-1. Total α-tubulin and acetylated tubulin localization appeared qualitatively similar in Nek8445 knockdown cells (Figure 4A), suggesting that microtubule organization was altered. Both antibodies stained nodes of tubulin at the tips of flagella in the Nek8445 knockdown cells suggesting a defect in flagella length homeostasis. Additionally, approximately 15% of the knockdown cells had both short flagella and a rounded cell shape. We noticed that these small cells lacked median bodies. Upon quantitation, we found that 46.8% (n=158) of all Nek8445 depleted cells lacked median bodies versus just under 15% (n=302) of the control cells. Note that this tubulin reservoir is consumed during mitosis and then grows in size as cells prepare for the next round of division (Hardin *et al.*, 2017; Horlock-Roberts *et al.*, 2017). Immunoblotting did not detect a significant difference in the ratio of acetylated to non-acetylated α-tubulin (Figure 4C), suggesting that Nek8445 does not regulate acetylation. The altered appearance of axoneme staining and the diminished number of cells with median bodies is consistent with major defects in microtubule array organization in *Giardia*.

**Nek8445 depleted cells have defective ventral disc organization**

We previously reported that Nek8445 depleted cells were defective in their ability to attach to the sidewalls of culture tubes (Hennessey *et al.*, 2016). Attachment is largely attributed to the microtubule-based suction cup-like organelle known as the ventral adhesive disc (Dawson and Nosala, 2017). Since the ventral disc failed to stain with tubulin antibodies in many of the Nek8445 depleted cells, we examined localization of the ventral disc marker δ-giardin to verify that a ventral disc was still present (Jenkins *et al.*, 2009; Halpern *et al.*, 2017). We did not find

any cells lacking δ-giardin staining, indicating that the ventral disc was present (Figure 5). However, we observed abnormal disc organization that correlated with abnormal cell shape and flagella length. Of the Nek8445 depleted cells that had short flagella and, therefore, had an impactful depletion of Nek8445, we observed that 38% of these cells had altered disc morphology including a larger area devoid of microtubule staining in the center of the disc (bare area), frayed and open disc conformations (Figure 5). Similar defects have been observed in cells depleted of disc associated proteins (DAPs) that have a structural role in the ventral disc (McInally *et al.*, 2018). The disc defect and overall changes in tubulin organization suggest Nek8445 has a role in regulating overall tubulin homeostasis.

**Nek8445 depleted cells have flagella exit defects**

In contrast to the typical half-pear shape of trophozoites, a subset of Nek8445 depleted cells were observed to have a rounded cell shape that lacked a portion of the posterior end of the cell. Tubulin staining indicated that the caudal flagella of these cells were either tucked under or folded within the cell body but this could not be resolved with light microscopy (Figure 4 and 5). To resolve whether the flagella were trapped in the trophozoite cell body we turned to Scanning Electron Microscopy (SEM). Control and Nek8445 depleted cells were processed for SEM 12 h after morpholino treatment. As observed by light microscopy, a subset of the Nek8445 depleted cells were much smaller and had short flagella. While the anterior, ventral and ventrolateral flagella were visible, the caudal flagella frequently did not exit from the cell body. In some cases, we could see abnormal membrane protrusions near where the caudal flagella were expected to exit, suggesting that Nek8445 depletion impairs flagella exit site specification (Figure 6 Arrowhead). This defect is expected to contribute to the cytokinesis defects observed with Nek8445 depletion as the flagella must be properly oriented in order to collaboratively generate forces for cytokinesis (Paredez *et al.*, 2011; Hardin *et al.*, 2017).

The defective flagella exit defect provided us with the opportunity to investigate whether the exit site is pre-determined or established after the flagella are in position. Unlike other

eukaryotes where basal body appendages known as transition fibers dock the basal body to the plasma membrane (Goncalves and Pelletier, 2017), *Giardia* basal bodies are positioned many microns from where flagella exit the cell body and become sheathed by plasma membrane. Giardia lacks all known transition zone proteins, so how the flagella exit site is specified remains an open question (Avidor-Reiss & Leroux, 2015; Barker, Renzaglia, Fry, & Dawe, 2014). A recent study of *Giardia* IFT suggests the exit sites are pore-like diffusion barriers that regulate intraflagellar transport (IFT) (McInally *et al.*, 2019). The Hehl lab, University of Zurich, fortuitously identified GL50803_8855 as a protein that forms a ring at the flagella exit site, where the axonemes transition from cytoplasmic to membrane sheathed (GiardiaDB). We endogenously tagged Exit Site Protein 8855 (ESP8555) with a triple HA tag to see if the exit site was somehow altered in the Nek8445 knockdown cells. As previously reported, we observed distinct localization of ESP8555-HA to the exit site of each flagella set in control cells (Figure 7). In Nek8445 knockdown cells, ESP8855 localization varied. In cells where the caudal flagella exited the cell body, ESP8855-HA was present where axonemes met the plasma membrane. However, ESP8855-HA did not mark the posterior exit site in severely rounded cells with extremely short caudal flagella, suggesting that the exit site is specified upon flagella contact with the plasma membrane (Figure 7).

**Super-Resolution Imaging reveals Nek8445 depleted cells lack a funis**

Nek8445 depletion alters the lengths of all flagella, but the caudal flagella were specifically susceptible to being trapped in the cell body without an exit site. Many of the trapped flagella are long enough to exit the cell body; therefore, the failure to exit cannot simply be attributed to length. What is unique about the caudal flagella is that they make the longest run through the cell body and they are sandwiched between the two halves of the funis (see Figure 1). Our initial imaging of Nek8445 depleted cells indicated that the axonemes stained with higher contrast which made us question if the funis was absent in these cells. The funis is difficult to observe with standard resolution microscopy, so we turned to structured illumination super-resolution

microscopy to compare control and Nek8445 depleted cells. We were able to resolve the funis in every control cell examined (n=12) while none of the rounded cells (n=12) had any vestige of a funis (Figure 8). Another unique feature of the rounded cells is that we observed several cells with frayed flagella tips, further suggesting an axoneme stability defect in Nek8445 depleted cells. Together this work illustrates the overall importance of Nek8445 in regulating the microtubule cytoskeleton of *Giardia*. The correlation of round cell shapes, defective flagella exit, and the lack of a funis is consistent with the funis having a role in establishing *Giardia* cell shape and guiding caudal flagella exit.

## Discussion

Characterization of the Nek8445 knockdown phenotypes illustrates a requirement for Nek8445 in coordinating microtubule organization essential for proper parasite attachment and cell division. This study reinforces our view that the microtubule cytoskeleton has expanded function for *Giardia* cell division which includes force generation necessary for cytokinesis (Hennessey *et al.*, 2016; Hardin *et al.*, 2017). Recent advances in live cell imaging have made it possible to visualize *Giardia* mitosis and cytokinesis with fantastic spatial-temporal resolution (Hardin *et al.*, 2017).

Our data suggests that the primary cause of cytokinesis defects that result from Nek8445 depletion can be attributed to defective flagella and highlights the importance of the flagella for *Giardia* cytokinesis. Our working model posits that at the onset of cytokinesis the caudal flagella, each connecting to a daughter ventral disc, orients the daughter discs so that the anterior-most regions face away from one another. Subsequently, power strokes from the anterior flagella drive the two daughter cells in opposite directions generating the membrane tension required for division (Zhang and Robinson, 2005; Ralston *et al.*, 2006; Poirier *et al.*, 2012; Hardin *et al.*, 2017). That we can observed outwardly normal looking cells, in terms of cell shape and flagella length, that fail cytokinesis suggests that the flagella may have improper function prior to shortening. Cytokinesis in these cells likely fails because the caudal axonemes

are not able to orient the daughter disks in opposition to each other (Fig 2 and Video S1). Knockdown cells with short flagella would additionally be unable to generate the normal amount of propulsion to drive daughter cells apart. An additional compounding factor is that Nek8445 depleted cells were frequently observed without median bodies. The lack of median bodies is an indicator of reduced tubulin reservoirs. During mitosis, tubulin fluxes from the median body, to the spindle, to the nascent disks and finally to the growing axonemes. Growth of the new axonemes could be impaired due to a limited tubulin supply, but the short flagella may also indicate a defect in IFT. Indeed, the short flagella phenotype observed in Nek8445 depleted cells is reminiscent of Kinesin-2 mutants which impair IFT (Hoeng *et al.*, 2008; Carpenter and Cande, 2009). Interestingly however, the trapped flagella eventually grow to lengths that appear longer than the flagella pairs that exit the cell body. This supports the notion that Giardia can employ IFT independent cytoplasmic axomene growth as cytoplasmic axonemes do not necessarily need active IFT for growth (Briggs *et al.*, 2004; McInally *et al.*, 2019).

A consequence of slow growing flagella could be the loss of the tracks that deliver membrane into the furrow (Hardin *et al.*, 2017), which could contribute to failed cytokinesis. Due to the lack of robust cell synchronization and the very short window in which cells use these tracks to deliver membrane, it is technically challenging to find knockdown cells actively dividing in order to test this hypothesis. Still, we reason that the short flagella phenotype observed in interphase cells is manifested in mitosis when the nascent flagella begin to assemble (Nohynkova *et al.*, 2006; Hardin *et al.*, 2017).

The caudal flagella exit defect provided a unique opportunity to probe the mechanism of exit site specification/flagella pore formation in *Giardia*. ESP8855 marks flagella exit sites. When Nek8445 was depleted, cells with extremely short flagella were observed to lack ESP8855 staining at the posterior apex of the cell, which is where the caudal flagella normally exit. This is consistent with axoneme contact with the plasma membrane being the specifier for exit site/flagella pore complex formation rather than the axoneme being targeted to a pre-

determined position on the membrane. Aberrant flagella exiting, as seen in Figure 6A, suggests a role for Nek8445 in regulating exit site specification; however, since only the caudal flagella were seen to have this defect it seems likely this is a secondary defect. The caudal flagella make the longest run through the cell body and are unique in their association with the axostyle or funis, a ribbon of microtubules that runs along the length the intracytoplasmic axoneme of each caudal flagellum (Benchimol *et al.*, 2004). The ribbon originates near the basal bodies and as it progresses toward the posterior, individual microtubules splay out to form rib like structures that match the shape of the cell (Figure 1, 8) (Benchimol *et al.*, 2004). A defect in flagella guidance could lead to defects in specifying the exit site if for example the flagella must remain in place for the flagella exit site to be assembled. Indeed, the flagella exit defect was specifically associated with rounded Nek8445 depleted cells which we found also lack funis microtubules (Fig 8). This suggests that the funis is a scaffold for guiding caudal flagella exit. The authors of ultrastructure studies have suggested axostyles play a role in organizing cell shape (Benchimol *et al.*, 2004; de Andrade Rosa *et al.*, 2013). Indeed, iron deficiency or treatment with the phosphatase inhibitor calyculin A leads to loss of axostyles and altered cell shape in Trichomonas (De Jesus *et al.*, 2007; Munoz *et al.*, 2012). Here we have identified the first protein that has a role in regulating axostyle formation adding to the list of functions regulated by Nek family kinases.

For an otherwise minimalistic parasite, the hugely expanded family of Nek kinases is intriguing. *Giardia* has 189 members compared with just one non-essential Nek Kinase in yeast, seven in *Arabidopsis*, and 11 in humans. Each of the three *Giardia* Nek kinases that have been studied appear to regulate different cellular processes. Depletion studies for GlNek1 and GlNek2 were not performed so whether they are required for cell division remains to be determined. However, localization studies did reveal that these proteins re-localized during mitosis and therefore they likely regulate the microtubule cytoskeleton in a cell cycle dependent manner (Smith *et al.*, 2012). *Giardia* lacks the Anaphase Promoting Complex (APC)

(Gourguechon *et al.*, 2013), which normally regulates cell cycle events through proteolytic degradation. It has been speculated that kinases could play an expanded role in regulating cell cycle related process in *Giardia* (Gourguechon *et al.*, 2013); the expanded Nek kinase family potentially fills this role. Future studies aimed at identifying pathways regulated by additional Nek kinases will be needed to further support this hypothesis. Given the total number of Nek kinases in *Giardia,* we would have anticipated each kinase to have a limited role in cytoskeletal regulation, yet Nek8445 depletion disrupts nearly every known microtubule structure in Giardia. We speculate that this is because Nek8445 regulates a key microtubule binding protein. Therefore, it will be interesting to identify Nek8445 phosphorylation targets to gain insight into microtubule array regulation in *Giardia*.

Whether many other Nek kinases play as critical a role as Nek8445 in cell division and microtubule array biogenesis remains to be determined, but the presence of a small gatekeeper residue in Nek8445 makes this protein kinase a particularly attractive drug target as this structural feature renders this kinase sensitive to bumped kinase inhibitors. Importantly, we have already shown this class of inhibitor is effective at killing parasites resistant to metronidazole (Hennessey *et al.*, 2016), the frontline treatment for giardiasis.

**Acknowledgements:**

We thank Christine Wong for technical assistance and Wai Pang for help with the SEM. We thank Elizabeth Thomas and Melissa Steele-Ogus for help with editing and preparing figures. This work was supported by NIH award R01AI110708 to A.R.P and R21AI127493 to E.A.M. The funders had no role in study design, data collection and interpretation, or the decision to submit the work for publication.

**Legends**

**Figure 1.** Diagram of *Giardia* emphasizing microtubule-based structures. The microtubule cytoskeleton includes the ventral disc, median body, funis, anterior, posteriolateral, ventral and

caudal flagella sets.

**Figure 2.** Nek8445 is required for cytokinesis. (A) Multiplex immunoblot showing Nek8445-HA depletion 12 and 24 hours after Nek8445 antisense and control morpholino treatment. (B) Representative still images from a 4D time-lapse movie showing failed cytokinesis in Nek8445 depleted cells (see Video S1). (C) Analysis of cytokinesis timing indicating that only 13% of Nek8445 depleted cells complete cytokinesis within 2 minutes while 48% are never able to complete cytokinesis. Scale bar = 5 µm.

**Figure 3.** Nek8445 re-localizes during mitosis to associate with the spindle and axoneme microtubules (A) Still images form time-lapse movie of Nek8445-mNG showing Nek8445 translocating from the cell cortex to the nuclear envelope, spindle, and axoneme microtubules (See Video S2). (B) Immuno-fluorescence analysis of Nek8445-HA (red), microtubules (green), and nuclei (DAPI, blue) throughout the cell cycle. Scale bar = 5 µm.

**Figure 4.** Nek8445 regulates microtubule organization. (A) Immunofluorescence staining of acetylated and total α-tubulin using anti-α-tubulin antibody DM1A (red) and the anti-acetylated α-tubulin antibody 6-11B-1 (green). Note changes in overall tubulin staining after Nek8445 depletion including reduced ventral disc (vd) staining, the lack of a median body (mb) in round cells, and nodes of tubulin staining at the ends of flagella. Scale bar = 5 µm. (B) Quantification of mutant phenotypes observed after Nek8445 depletion. (C) Immunoblotting for total tubulin (DM1A) vs acetylated tubulin (6-11-B1) in Nek8445 and control morpholino cells does not indicate a change in acetylation levels although overall tubulin levels are decreased by ~25%.

**Figure 5.** Nek8445 depleted cells have ventral disc organization defects. Control and Nek8445 knockdown cells stained for Delta Giardin and tubulin (6-11B-1). Note the altered disc

morphology such as increased width, larger bare area, and some striated staining of Delta giardin not observed in control cells. Scale bar = 5 µm.

**Figure 6.** SEM analysis reveals Nek8445 depleted cells have flagella exit defects. Control and Nek8445 knockdown cells imaged with scanning electron microscopy eight hours after morpholino treatment. Note the shorter cell length and absence of caudal flagella exiting the anterior apex of the cell. White arrowhead indicates an abnormal membrane protrusion associated with a caudal flagellum that eventually exits the cell body at an abnormal position. Scale bar = 5 µm.

**Figure 7.** Nek8445 depleted cells with short caudal flagella lack exit sites. Control and Nek8445 knockdown cells were stained for tubulin and ESP8855. Representative knockdown cells are arranged from moderate to severe caudal flagella shortening. Note the lack of ESP8855 staining in the knockdown cell with extremely short caudal flagella (bottom image). Scale bar = 5 µm.

**Figure 8.** Structured Illumination super-resolution imaging reveals that Nek8445 depleted cells lack median bodies, a funis, and the flagella have a fraying defect. Control inset shows magnified view of funis microtubules. Middle inset shows that the Nek8445 depleted cells lack both a median body and funis. The bottom image shows an example of a Nek8445 depleted cell with abnormal disc morphology and splayed flagella tips.
Scale bar = 5 µm.

**Figure S1.** Rab11 and Nek8445 localization throughout the cell cycle. HA-Rab11 in cyan, Nek8445-mNG in red, and tubulin (6-11-B1) in green. Note that Nek8445 loads onto microtubule structures such as the spindle and axonemes during mitosis. Rab11 loads onto intracellular axonemes at specific times during mitosis, but Rab11 and Nek8445 are not frequently observed

to co-localize. White arrowhead shows an example of HA-Rab11 and Nek8445-mNG co-localization on the internal axonemes of the posterolateral flagella.

Video S1 Control and Nek8445 morpholino knockdown cells undergoing mitosis and cytokinesis. Note that the videos have been synchronized by the start of mitosis as indicated by anterior flagella re-organization.

Video S2 Live imaging of Nek8445-mNG during mitosis and cytokinesis.


Benchimol, M., Piva, B., Campanati, L., and de Souza, W. (2004). Visualization of the Funis of Giardia Lamblia by High-Resolution Field Emission Scanning Electron Microscopy--New Insights. J Struct Biol *147*, 102-115.

Bradley, B.A., and Quarmby, L.M. (2005). A Nima-Related Kinase, Cnk2p, Regulates Both Flagellar Length and Cell Size in Chlamydomonas. J Cell Sci *118*, 3317-3326.

Briggs, L.J., Davidge, J.A., Wickstead, B., Ginger, M.L., and Gull, K. (2004). More Than One Way to Build a Flagellum: Comparative Genomics of Parasitic Protozoa. Current biology : CB *14*, R611-612.

Carpenter, M.L., and Cande, W.Z. (2009). Using Morpholinos for Gene Knockdown in Giardia Intestinalis. Eukaryot Cell *8*, 916-919.

Chang, J., Baloh, R.H., and Milbrandt, J. (2009). The Nima-Family Kinase Nek3 Regulates Microtubule Acetylation in Neurons. J Cell Sci *122*, 2274-2282.

Dawson, S.C., and Nosala, C. (2017). The Ventral Disc Is a Flexible Microtubule Organelle That Depends on Domed Ultrastructure for Functional Attachment of Giardia Lamblia. bioRxiv.

de Andrade Rosa, I., de Souza, W., and Benchimol, M. (2013). High-Resolution Scanning Electron Microscopy of the Cytoskeleton of Tritrichomonas Foetus. J Struct Biol *183*, 412-418.

De Jesus, J.B., Cuervo, P., Junqueira, M., Britto, C., Silva-Filho, F.C., Soares, M.J., Cupolillo, E., Fernandes, O., and Domont, G.B. (2007). A Further Proteomic Study on the Effect of Iron in the Human Pathogen Trichomonas Vaginalis. Proteomics *7*, 1961-1972.

Goncalves, J., and Pelletier, L. (2017). The Ciliary Transition Zone: Finding the Pieces and Assembling the Gate. Molecules and cells *40*, 243-253.

Gourguechon, S., and Cande, W.Z. (2011). Rapid Tagging and Integration of Genes in Giardia Intestinalis. Eukaryot Cell *10*, 142-145.

Gourguechon, S., Holt, L.J., and Cande, W.Z. (2013). The Giardia Cell Cycle Progresses Independently of the Anaphase-Promoting Complex. Journal of Cell Science *126*, 2246-2255.

Halpern, A.R., Alas, G.C.M., Chozinski, T.J., Paredez, A.R., and Vaughan, J.C. (2017). Hybrid Structured Illumination Expansion Microscopy Reveals Microbial Cytoskeleton Organization. ACS nano *11*, 12677-12686.

Hardin, W.R., Li, R., Xu, J., Shelton, A.M., Alas, G.C.M., Minin, V.N., and Paredez, A.R. (2017). Myosin-Independent Cytokinesis in Giardia Utilizes Flagella to Coordinate Force Generation and Direct Membrane Trafficking. Proc Natl Acad Sci U S A.

Hennessey, K.M., Smith, T.R., Xu, J.W., Alas, G.C., Ojo, K.K., Merritt, E.A., and Paredez, A.R. (2016). Identification and Validation of Small-Gatekeeper Kinases as Drug Targets in Giardia Lamblia. PLoS neglected tropical diseases *10*, e0005107.

Hoeng, J.C., Dawson, S.C., House, S.A., Sagolla, M.S., Pham, J.K., Mancuso, J.J., Lowe, J., and Cande, W.Z. (2008). High-Resolution Crystal Structure and in Vivo Function of a Kinesin-2 Homologue in Giardia Intestinalis. Mol Biol Cell *19*, 3124-3137.

Horlock-Roberts, K., Reaume, C., Dayer, G., Ouellet, C., Cook, N., and Yee, J. (2017). Drug-Free Approach to Study the Unusual Cell Cycle of Giardia Intestinalis. mSphere *2*.

Janke, C., and Montagnac, G. (2017). Causes and Consequences of Microtubule Acetylation. Current biology : CB *27*, R1287-r1292.

Jenkins, M.C., O'Brien, C.N., Murphy, C., Schwarz, R., Miska, K., Rosenthal, B., and Trout, J.M. (2009). Antibodies to the Ventral Disc Protein Delta-Giardin Prevent in Vitro Binding of Giardia Lamblia Trophozoites. The Journal of parasitology *95*, 895-899.

Keister, D.B. (1983). Axenic Culture of Giardia-Lamblia in Tyi-S-33 Medium Supplemented with Bile. Transactions of the Royal Society of Tropical Medicine and Hygiene *77*, 487-488.

Keyloun, K.R., Reid, M.C., Choi, R., Song, Y., Fox, A.M.W., Hillesland, H.K., Zhang, Z., Vidadala, R., Merritt, E.A., Lau, A.O.T., Maly, D.J., Fan, E., Barrett, L.K., Van Voorhis, W.C., and Ojo, K.K. (2014). The Gatekeeper Residue and Beyond: Homologous Calcium-Dependent Protein Kinases as Drug Development Targets for Veterinarian Apicomplexa Parasites. Parasitology *141*, 1499-1509.

Lenaghan, S.C., Davis, C.A., Henson, W.R., Zhang, Z., and Zhang, M. (2011). High-Speed Microscopic Imaging of Flagella Motility and Swimming in Giardia Lamblia Trophozoites. Proc Natl Acad Sci U S A *108*, E550-558.

Manning, G., Reiner, D.S., Lauwaet, T., Dacre, M., Smith, A., Zhai, Y., Svard, S., and Gillin, F.D. (2011). The Minimal Kinome of Giardia Lamblia Illuminates Early Kinase Evolution and Unique Parasite Biology. Genome biology *12*, R66.

McInally, S., Kondev, J., and Dawson, S.C. (2019). Length-Dependent Disassembly Maintains Four Different Flagellar Lengths in <Em>Giardia</Em>. bioRxiv, 647115.

McInally, S.G., Hagen, K.D., Nosala, C., Williams, J., Nguyen, K., Booker, J., Jones, K., and Dawson, S.C. (2018). Robust and Stable Transcriptional Repression in Giardia Using Crispri. bioRxiv.

Munoz, C., Perez, M., Orrego, P.R., Osorio, L., Gutierrez, B., Sagua, H., Castillo, J.L., Martinez-Oyanedel, J., Arroyo, R., Meza-Cervantez, P., da Silveira, J.F., Midlej, V., Benchimol, M., Cordero, E., Morales, P., Araya, J.E., and Gonzalez, J. (2012). A Protein Phosphatase 1 Gamma (Pp1gamma) of the Human Protozoan Parasite Trichomonas Vaginalis Is Involved in Proliferation and Cell Attachment to the Host Cell. Int J Parasitol *42*, 715-727.

Nohynkova, E., Tumova, P., and Kulda, J. (2006). Cell Division of Giardia Intestinalis: Flagellar Developmental Cycle Involves Transformation and Exchange of Flagella between Mastigonts of a Diplomonad Cell. Eukaryot Cell *5*, 753-761.
Nosala, C., Hagen, K.D., and Dawson, S.C. (2018). 'Disc-O-Fever': Getting Down with Giardia's Groovy Microtubule Organelle. Trends Cell Biol *28*, 99-112.
O'Connell, M.J., Krien, M.J., and Hunter, T. (2003). Never Say Never. The Nima-Related Protein Kinases in Mitotic Control. Trends Cell Biol *13*, 221-228.
Paredez, A.R., Assaf, Z.J., Sept, D., Timofejeva, L., Dawson, S.C., Wang, C.J., and Cande, W.Z. (2011). An Actin Cytoskeleton with Evolutionarily Conserved Functions in the Absence of Canonical Actin-Binding Proteins. Proc Natl Acad Sci U S A *108*, 6151-6156.
Parker, J.D., Bradley, B.A., Mooers, A.O., and Quarmby, L.M. (2007). Phylogenetic Analysis of the Neks Reveals Early Diversification of Ciliary-Cell Cycle Kinases. PloS one *2*, e1076.
Poirier, C.C., Ng, W.P., Robinson, D.N., and Iglesias, P.A. (2012). Deconvolution of the Cellular Force-Generating Subsystems That Govern Cytokinesis Furrow Ingression. Plos Computational Biology *8*.
Ralston, K.S., Lerner, A.G., Diener, D.R., and Hill, K.L. (2006). Flagellar Motility Contributes to Cytokinesis in Trypanosoma Brucei and Is Modulated by an Evolutionarily Conserved Dynein Regulatory System. Eukaryot. Cell *5*, 696-711.
Rotella, D.P. (2012). Recent Results in Protein Kinase Inhibition for Tropical Diseases. Bioorganic & medicinal chemistry letters *22*, 6788-6793.
Shaner, N.C., Lambert, G.G., Chammas, A., Ni, Y., Cranfill, P.J., Baird, M.A., Sell, B.R., Allen, J.R., Day, R.N., Israelsson, M., Davidson, M.W., and Wang, J. (2013). A Bright Monomeric Green Fluorescent Protein Derived from Branchiostoma Lanceolatum. Nature methods *10*, 407-409.
Smith, A.J., Lauwaet, T., Davids, B.J., and Gillin, F.D. (2012). Giardia Lamblia Nek1 and Nek2 Kinases Affect Mitosis and Excystation. Int J Parasitol *42*, 411-419.
Takatani, S., Otani, K., Kanazawa, M., Takahashi, T., and Motose, H. (2015). Structure, Function, and Evolution of Plant Nima-Related Kinases: Implication for Phosphorylation-Dependent Microtubule Regulation. Journal of plant research *128*, 875-891.
Zhang, W., and Robinson, D.N. (2005). Balance of Actively Generated Contractile and Resistive Forces Controls Cytokinesis Dynamics. Proc Natl Acad Sci U S A *102*, 7186-7191.

**Figure1**

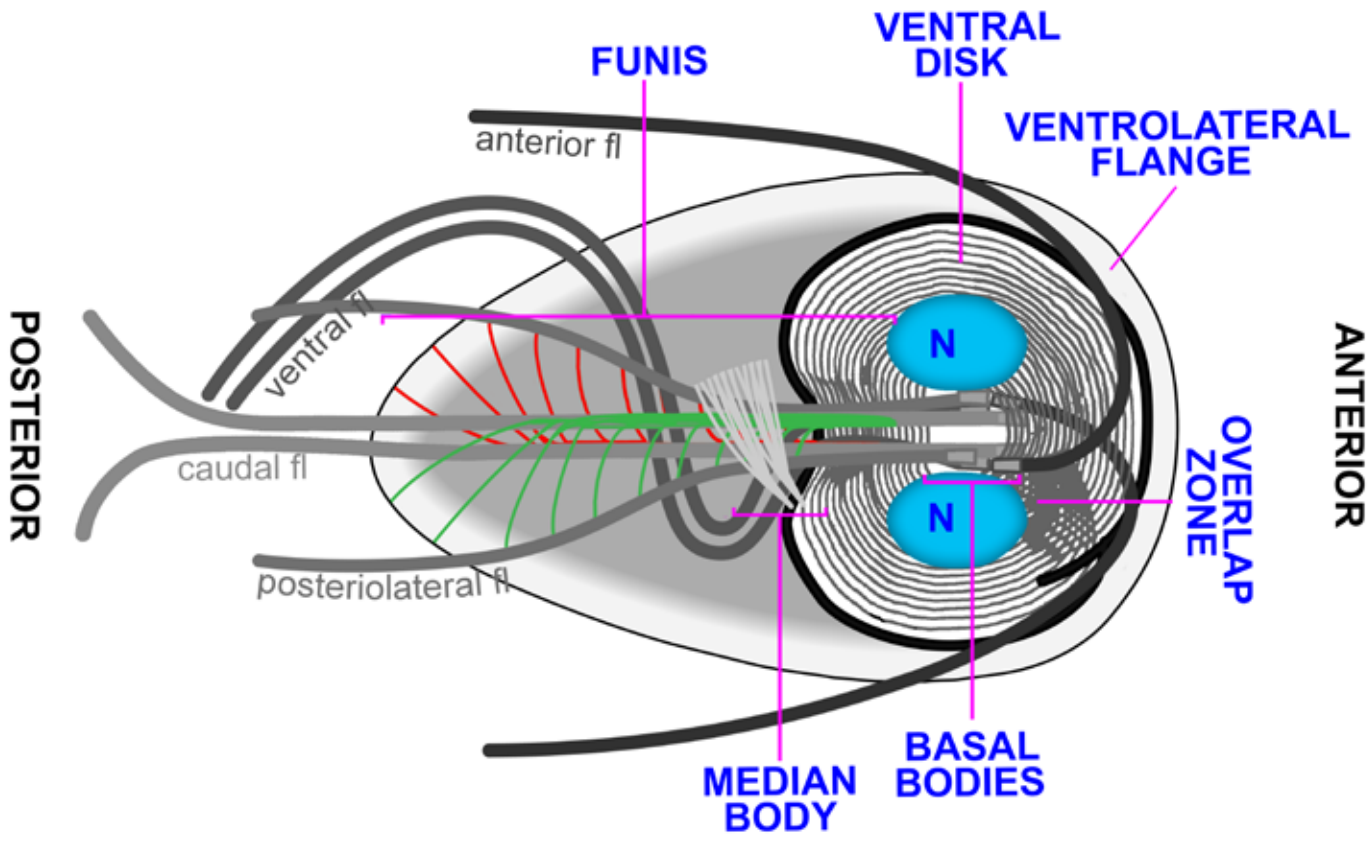


Figure 1. Diagram of Giardia emphasizing microtubule-based structures. The microtubule cytoskeleton includes the ventral disc, median body, funis, anterior, posteriolateral, ventral and caudal flagella sets.

# Figure 2

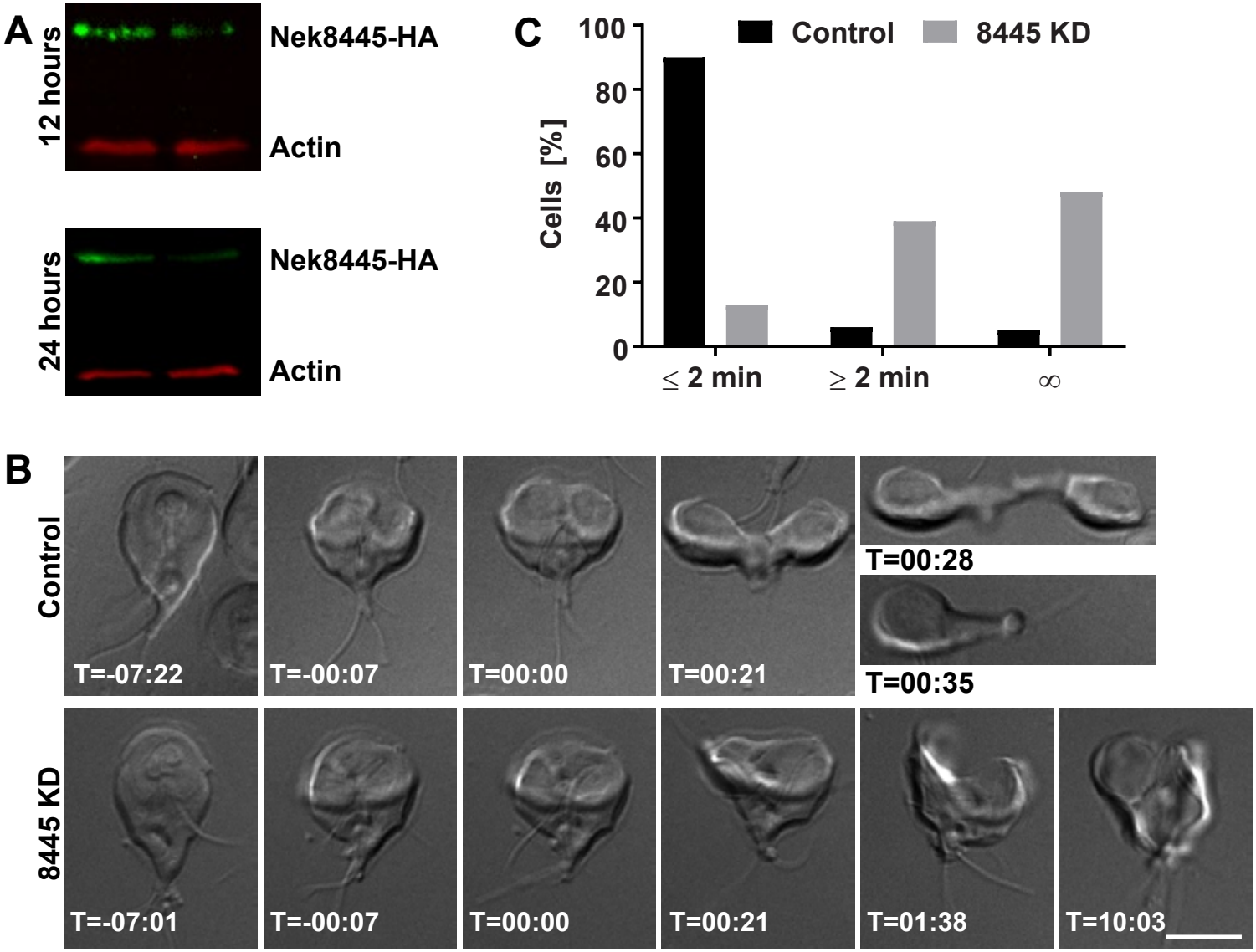


Figure 2. Nek8445 is required for cytokinesis. (A) Multiplex immunoblot showing Nek8445-HA depletion 12 and 24 hours after Nek8445 antisense and control morpholino treatment. (B) Representative still images from a 4D time-lapse movie showing failed cytokinesis in Nek8445 depleted cells (see Video S1). (C) Analysis of cytokinesis timing indicating that only 13% of Nek8445 depleted cells complete cytokinesis within 2 minutes while 48% are never able to complete cytokinesis. Scale bar = 5 µm.

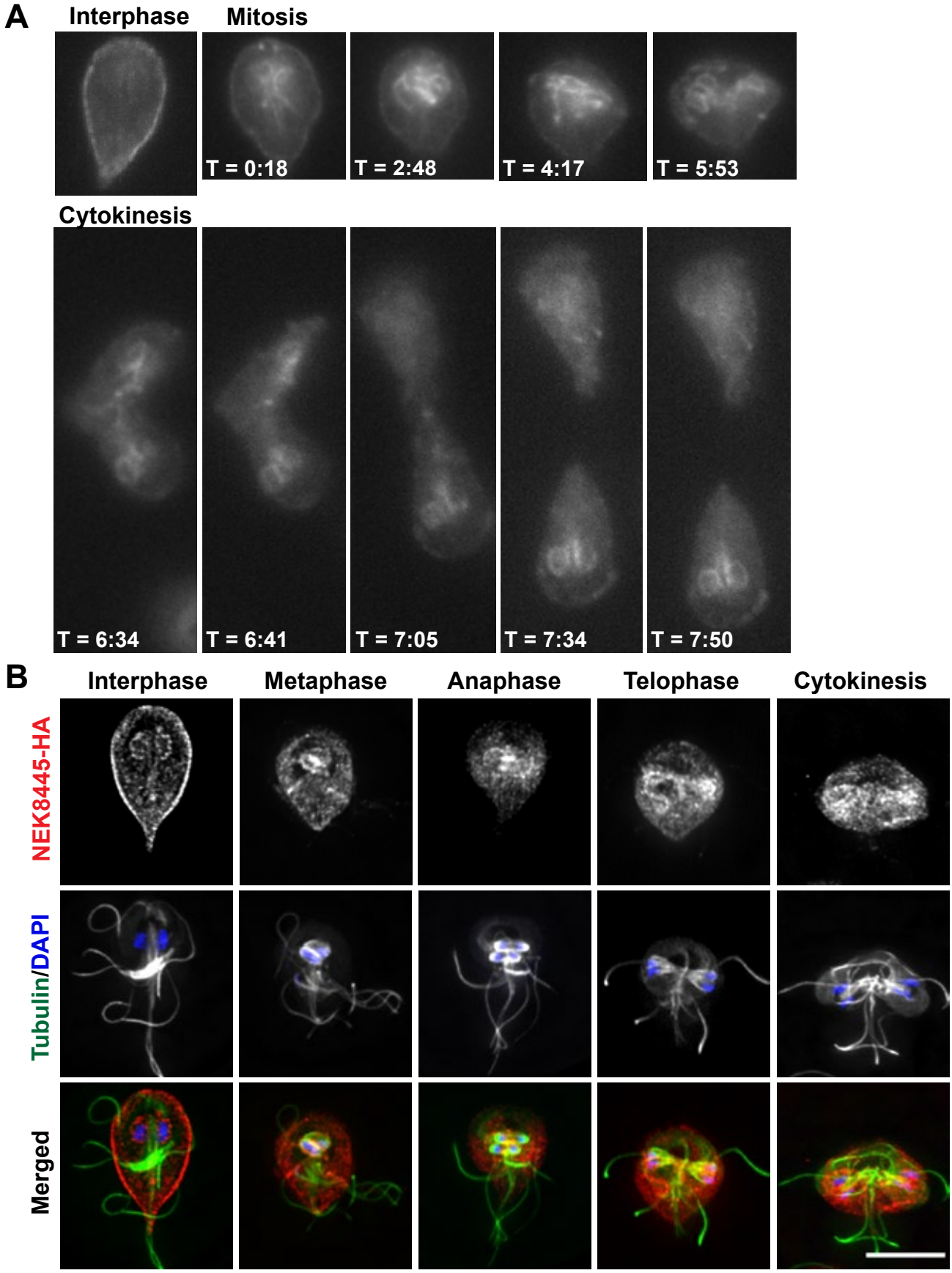


Figure 3

Figure 3. Nek8445 re-localizes during mitosis to associate with the spindle and axoneme microtubules (A) Still images form time-lapse movie of Nek8445-mNG showing Nek8445 translocating from the cell cortex to the nuclear envelope, spindle, and axoneme microtubules (See Video S2). (B) Immuno-fluorescence analysis of Nek8445-HA (red), microtubules (green), and nuclei (DAPI, blue) throughout the cell cycle. Scale bar = 5 µm.

# Figure 4

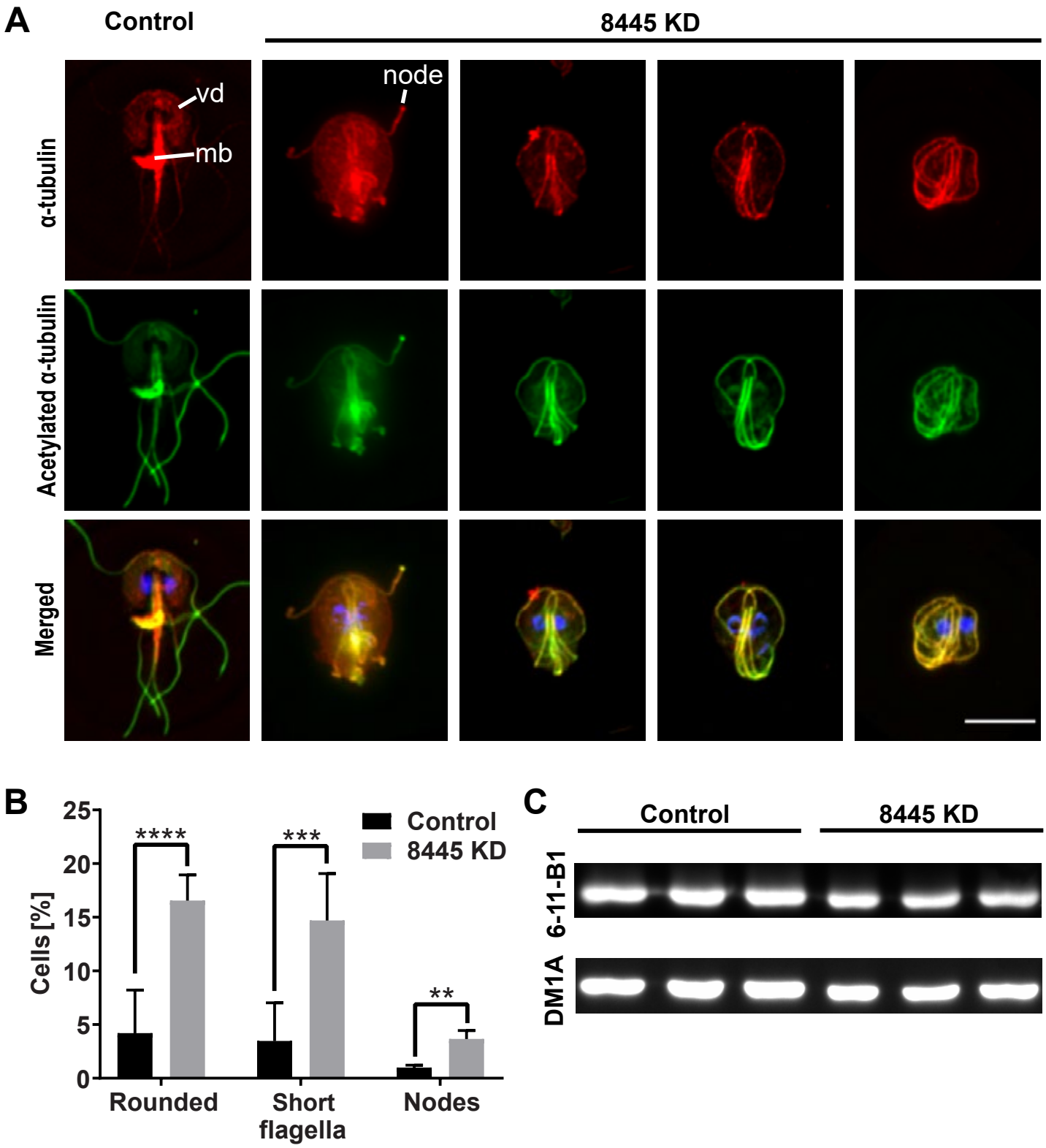


Figure 4. Nek8445 regulates microtubule organization. (A) Immunofluorescence staining of acetylated and total α-tubulin using anti-α-tubulin antibody DM1A (red) and the anti-acetylated α-tubulin antibody 6-11B-1 (green). Note changes in overall tubulin staining after Nek8445 depletion including reduced ventral disc (vd) staining, the lack of a median body (mb) in round cells, and nodes of tubulin staining at the ends of flagella. Scale bar = 5 µm. (B) Quantification of mutant phenotypes observed after Nek8445 depletion. (C) Immunoblotting for total tubulin (DM1A) vs acetylated tubulin (6-11-B1) in Nek8445 and control morpholino cells does not indicate a change in acetylation levels although overall tubulin levels are decreased by ~25%.

# Figure 5

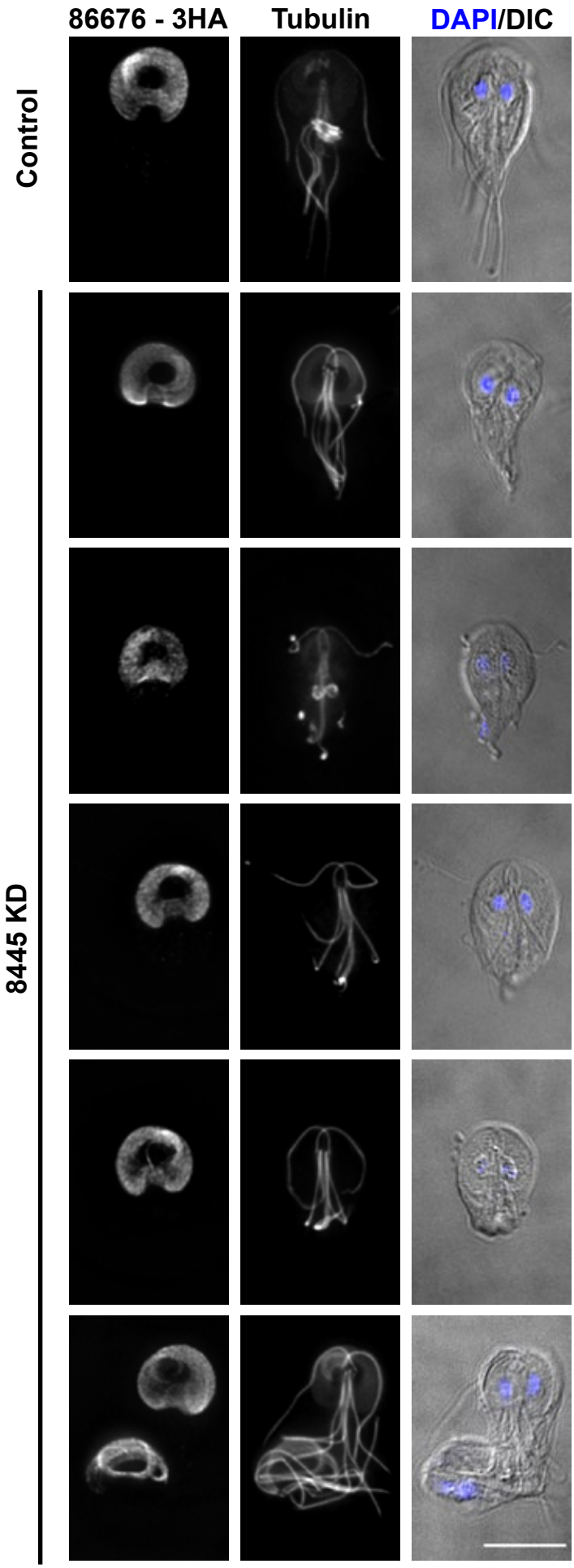


Figure 5. Nek8445 depleted cells have ventral disc organization defects. Control and Nek8445 knockdown cells stained for Delta Giardin and tubulin (6-11B-1). Note the altered disc morphology such as increased width, larger bare area, and some striated staining of Delta giardin not observed in control cells. Scale bar = 5 µm.

# Figure 6

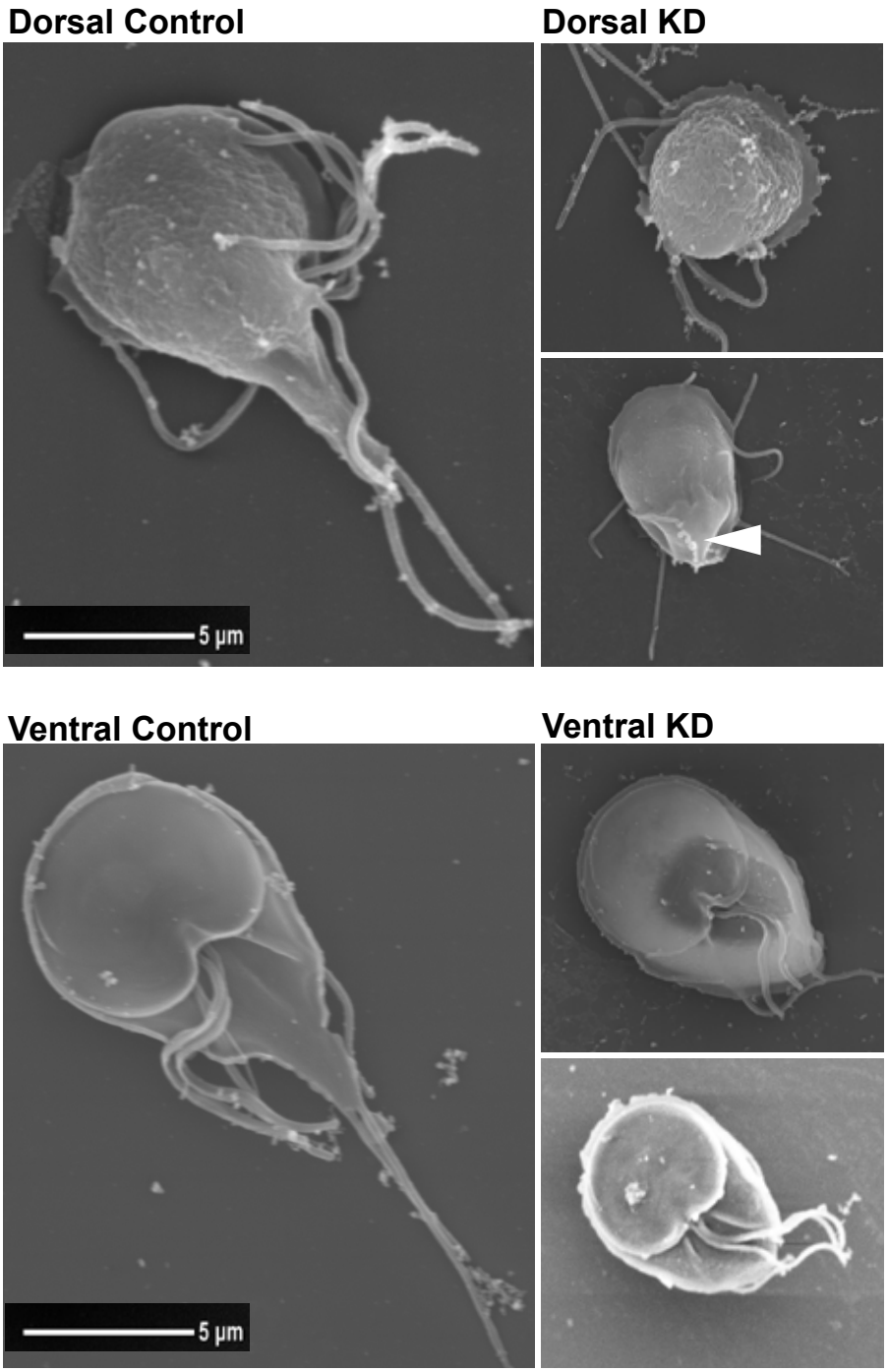


**Figure 6.** SEM analysis reveals Nek8445 depleted cells have flagella exit defects. Control and Nek8445 knockdown cells imaged with scanning electron microscopy eight hours after morpholino treatment. Note the shorter cell length and absence of caudal flagella exiting the anterior apex of the cell. White arrowhead indicates an abnormal membrane protrusion associated with a caudal flagellum that eventually exits the cell body at an abnormal position. Scale bar = 5 µm.

# Figure 7

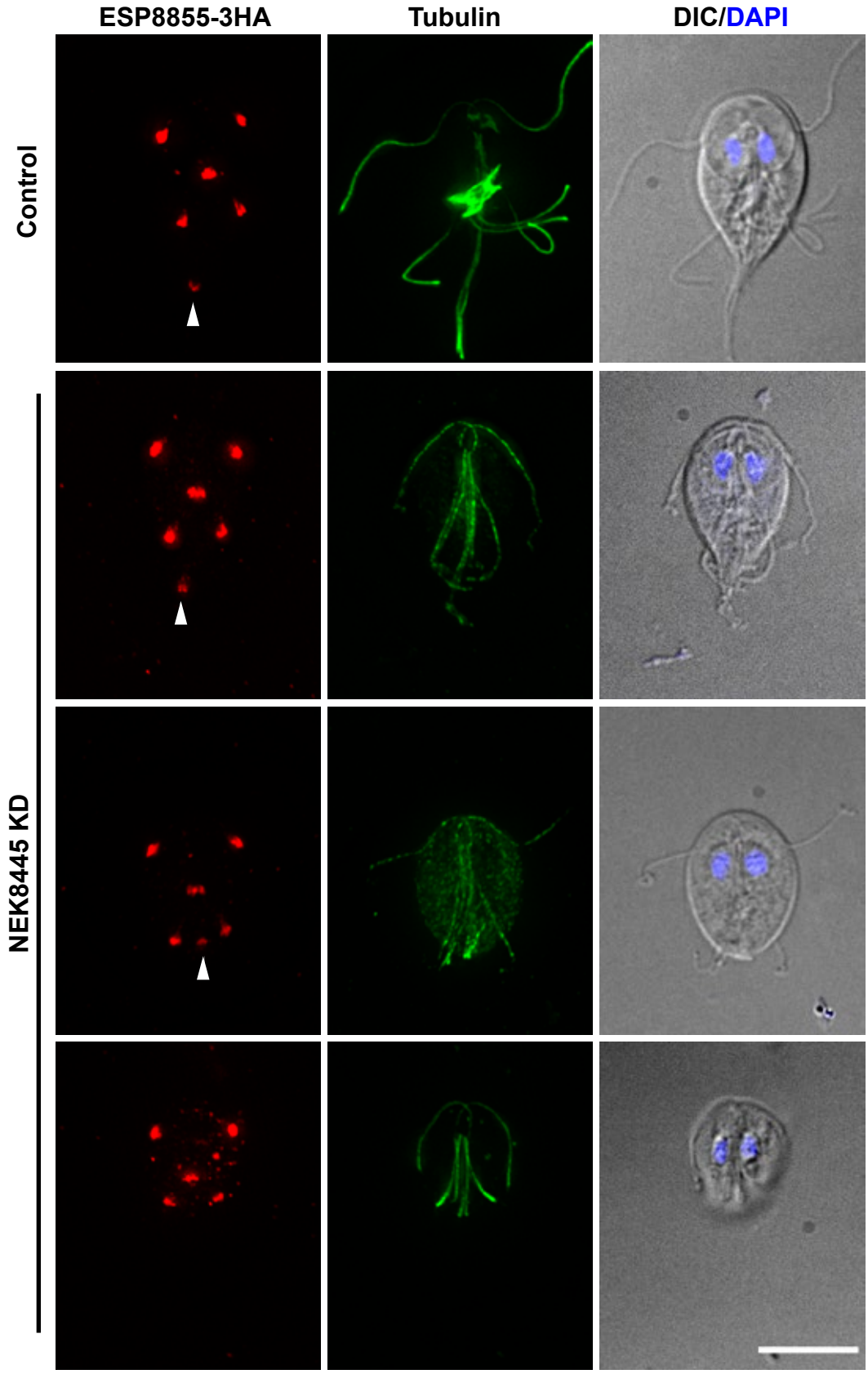


**Figure 7.** Nek8445 depleted cells with short caudal flagella lack exit sites. Control and Nek8445 knockdown cells were stained for tubulin and ESP8855. Representative knockdown cells are arranged from moderate to severe caudal flagella shortening. Note the lack of ESP8855 staining in the knockdown cell with extremely short caudal flagella (bottom image). Scale bar = 5 µm.

# Figure 8

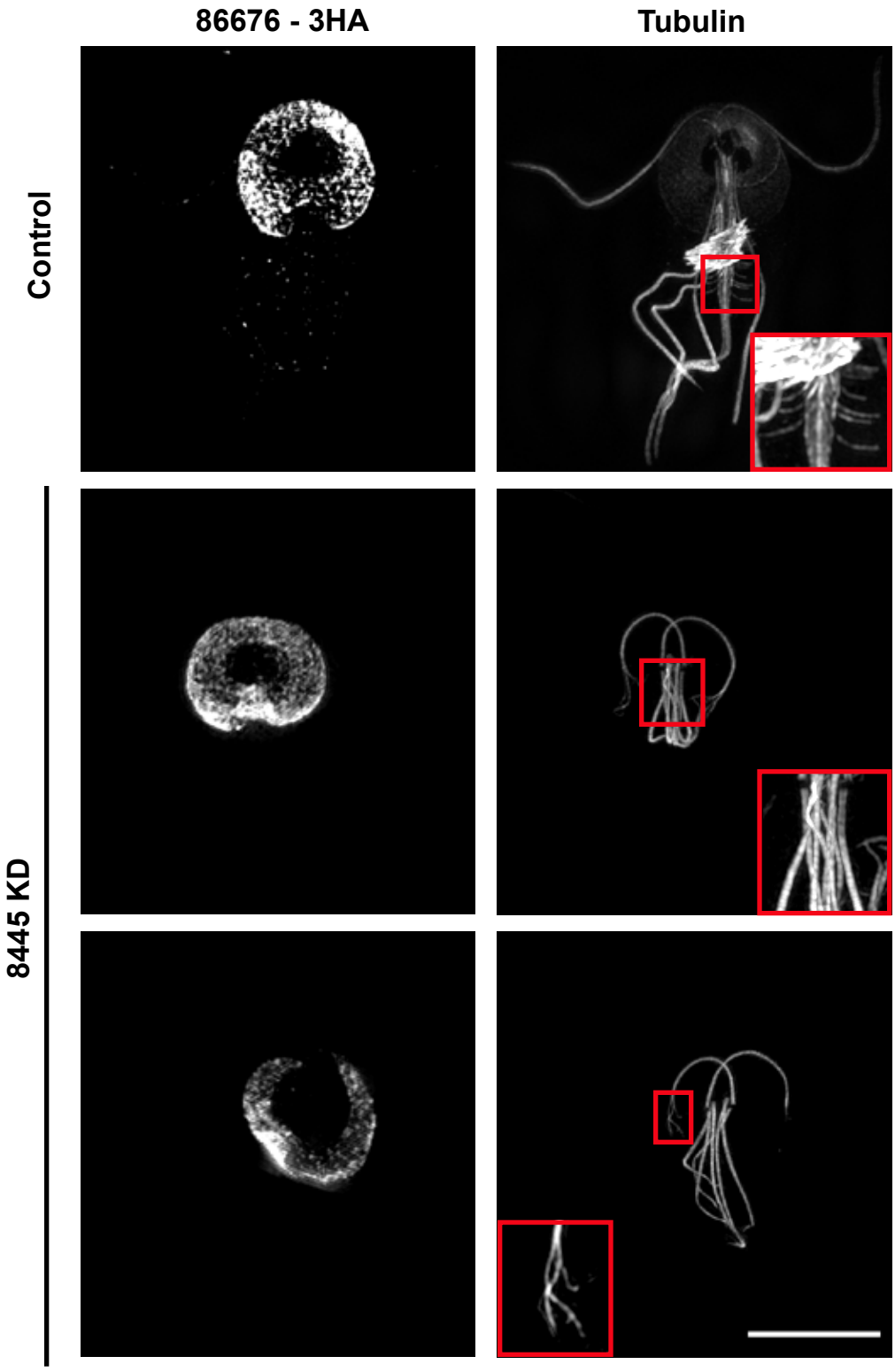


**Figure 8.** Structured Illumination super-resolution imaging reveals that Nek8445 depleted cells lack median bodies, a funis, and the flagella have a fraying defect. Control inset shows magnified view of funis microtubules. Middle inset shows that the Nek8445 depleted cells lack both a median body and funis. The bottom image shows an example of a Nek8445 depleted cell with abnormal disc morphology and splayed flagella tips.

Scale bar = 5 μm.

# Figure S1

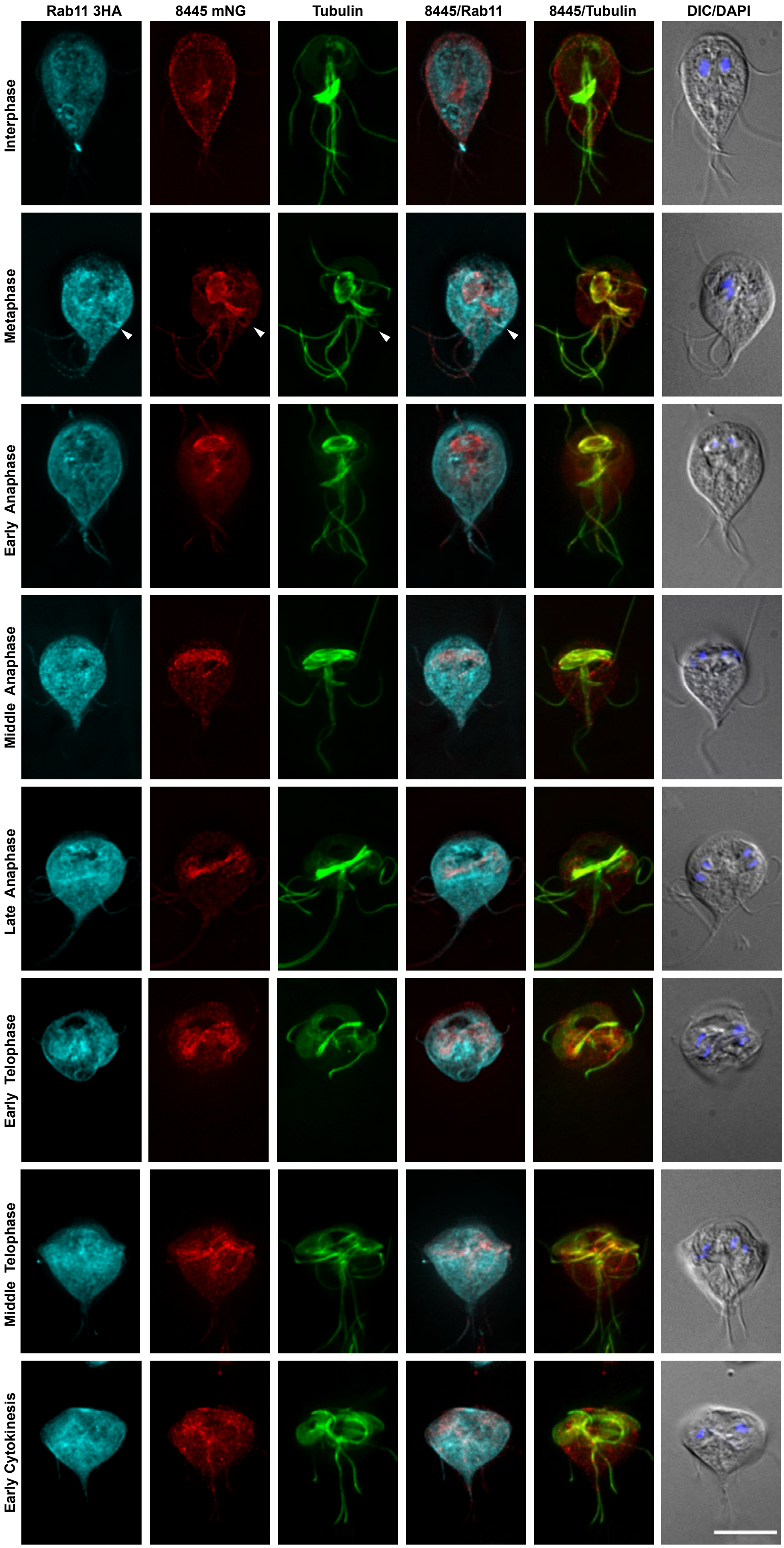


Figure S1. Rab11 and Nek8445 localization throughout the cell cycle. HA-Rab11 in cyan, Nek8445-mNG in red, and tubulin (6-11-B1) in green. Note that Nek8445 loads onto microtubule structures such as the spindle and axonemes during mitosis. Rab11 loads onto intracellular axonemes at specific times during mitosis, but Rab11 and Nek8445 are not frequently observed to co-localize. White arrowhead shows an example of HA-Rab11 and Nek8445-mNG co-localization on the internal axonemes of the posterolateral flagella.

| PRIMER NAME | RESTRICTION ENZYME | 5’ TO 3’ SEQUENCE |
|---|---|---|
| 8445_VSVG_Neo R | AgeI | TTCAATATCAGTATAaccggtcttgttgttagtctgtagccat |
| 8445_VSVG_Neo F | NotI | tggagctccaccgcggtggcggccgcCATAATCTTGGCGTCCTTCG |
| 8445_mNG_Neo F | NotI | ctccaccgcggtggcggccgcCATAATCTTGGCGTCCTTCG |
| 8445_mNG_Neo R | BamHI | AACCGCCTCCGGATCCCTTGTTGTTAGTCTGTAGCC |
| 8855_3HA_Neo F | SpeI | cggtggcggccgctctagaactagtTGTTGAGGTATCTGGGGATATT |
| 8855_3HA_Neo R | AflII | gtcataaggatattccttaagAATATCAAAATCGTCGAAATCACC |
| pks_mNG_NEO_F | BamHI | cggccgctctagaactagtggatccGGAGGCGGTTCAGGCGGAGG TGGCTCTatggtgagcaagggcgagga |
| pks_mNG_NEO_R | EcoRI | Gcaacgatgatgcaaagaattcttacttgtacagctcgtccatg |
| | | |
| Morpholino | | |
| 8445 | | CTGCCAGCTTCTCCGCAATACCCAT |

Table S1 Oligo sequences used in this study